Reversible structural change and thermodynamic properties of hydrogen in thin vanadium films

J. Bloch,* B. Hjörvarsson, S. Olsson, and R. Brukas
Department of Physics, University of Uppsala, Box 530, SE-75121, Uppsala, Sweden
(Received 1 December 2006; revised manuscript received 22 February 2007; published 27 April 2007)

The absorption of H in 50 nm V(001) films under pressures of $1-10^4$ Pa H_2 and at temperatures between 310 and 530 K was studied using *in situ* combined x-ray diffraction (XRD) and electrical resistivity measurements. The H-induced XRD peak shifts clearly indicate a fully reversible and nondeteriorating first-order phase transformation for the film. The H-induced residual resistivity changes in the V film demonstrate several extreme points (maxima and minima) apparently associated with some special points on the pressure isotherms of the film both below and above the critical temperature ($T_c=460\pm20$ K). Correlating these extreme points with the known V(bulk)-H phase diagram indicates that, in addition to the first-order transformation, two additional reversible second-order transitions exist in the film. The enthalpy and entropy of this transformation, obtained from the temperature dependence of the plateau pressures, are -39 ± 1 kJ/mol°K, and -60 ± 2 J/mol, respectively. The thermodynamic constants and the lattice parameters of the phases for the first-order transformation in the film closely correspond to the $\alpha\rightarrow\beta$ phase transformation in bulk V.

DOI: 10.1103/PhysRevB.75.165418 PACS number(s): 68.47.De

I. INTRODUCTION

Hydrogen reacts readily with the metals of group V (Nb, Ta, and V), in which the hydrogen is located interstitially, yielding a variety of structures.[1,2] The thermodynamics of a *M*-H system (where *M* is a hydride-forming metal) is strongly affected by the shape as well as the structure. For example, amorphous or glassy states, nanostructures, thin films and multilayers, and of course the bulk material all have their features as reflected by, e.g., the thermodynamic properties. Thus, both the crystalline ordering as well as the physical shape of the absorbing material affect the uptake.

The interaction of thin films and multilayers of group-V metals with hydrogen has been extensively studied during the last three decades.[3] When comparing the thermodynamic properties of hydrogen in thin films of these metals with the bulk material, significant differences are revealed. For example, the solubility of hydrogen in thin Nb-Ta(110) superlattices is dramatically increased as compared with the solubility in bulk Nb or Ta.[4] For thin epitaxial Nb(110) films, on the other hand, the hydrogen solubility is considerably reduced compared to that in bulk Nb.[5] Similarly, the hydrogen absorption in the vanadium layers in Mo/V(001) (Ref. 6) and Fe/V(001) (Ref. 7) superlattices strongly depends on the layer thickness of both the constituents. Furthermore, the critical temperature T_c depends strongly on the film thickness. For example, the critical temperature of the $\alpha\rightarrow\alpha'$ phase transition in Nb(110) decreases with decreasing film thickness.[8,9] It is noteworthy that most of the research in hydrogen absorption in thin films and multilayers is limited to the range above the critical temperature. The reason for this restriction is that thin epitaxial as well as polycrystalline metallic films may be severely damaged due to the large volume and structure changes associated with a phase transition. Damage is already visible upon cycling films under hydrogen absorption and desorption within a single phase. Highly adhesive thin films, in contrast to the bulk metal, are not free to expand, due to the elastic boundaries provided by the substrates. Since the films are clamped to a rigid substrate, the in-plane expansion is limited and the films can only expand reversibly along the out-of-plane direction. For relatively low hydrogen concentrations (α phase) of the group-V metals, hydrogen resides in tetrahedral interstitials of the bcc metallic lattice.[1] In the bulk form, the hydrogen absorption induces linear isotropic expansion of the measured lattice parameter. Such an isotropic expansion is impossible for a film, due to the elastic boundaries provided by the substrate, which leads to a highly anisotropic lattice response. For Nb(110) on sapphire, for example, an out-of-plane expansion almost four times bigger than the bulk value,[10] and an in-plane compressive strain exceeding by at least a factor of 10 the elastic limit of the bulk metal,[11] were observed.

In both the β and α phases of Nb and Ta, hydrogen occupies tetrahedral sites.[1,2] However, the transition involves a considerable volume change[1] and the expansion is energetically costly in a clamped thin film, due to the restoring elastic forces. Consequently, the α-β transition is suppressed and no precipitation of these more concentrated phases could be observed[12] at relatively high concentrations. Furthermore, when an α-β transition is enforced in thin films of Nb, irreversible structural changes are observed.[5,9,13]

Preferential octahedral (O) occupation, as compared to tetrahedral (T) sites, is observed with decreasing lattice parameter in bcc structures.[14] This effect allows for a dual (O and T) site occupancy in the α phase of vanadium. Indeed, up to 10% of the deuterium occupies octahedral sites in the α phase of V.[15,16] The application of uniaxial stress can also trigger the occupation of O sites.[17]

In contrast to Nb and Ta, the hydrogen atoms enter the octahedral (O_z) sites of the vanadium body-centered tetragonal (bct) hydride phases. Comparing the lattice constants of α-vanadium and β-hydride shows large tetragonal distortion. c_0 of the β phase is expanded by 9% whereas the contraction of the basis axis a_0 of the bct structure is less than 1.2%.[18,19] The large anisotropic strain makes hydrogen atoms in the O_z sites sensitive to uniaxial stress compared with the T sites (Nb and Ta hydrides), the nearly isotropic strain of which

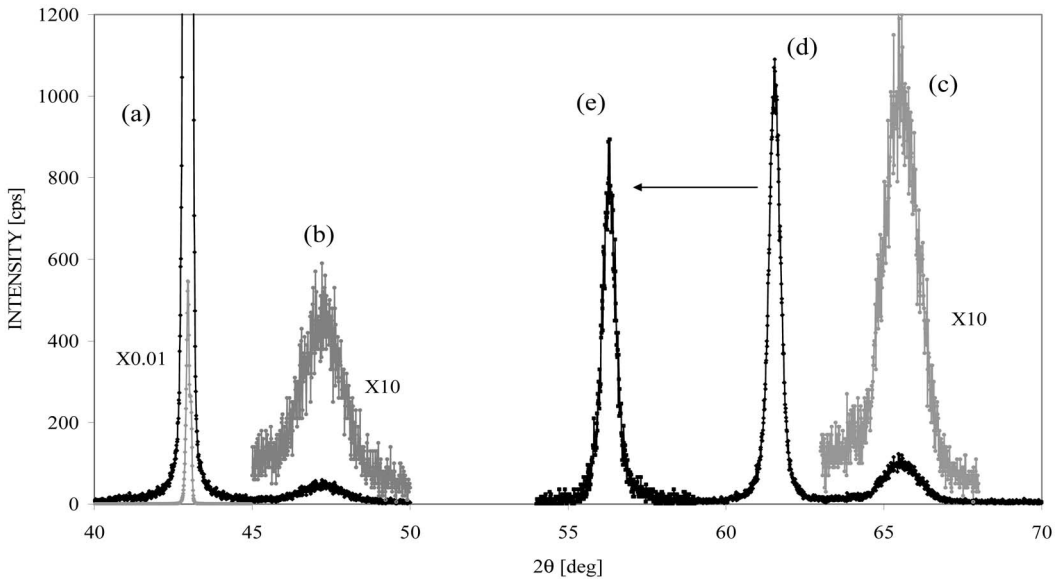

FIG. 1. XRD spectrum of the 50 nm V film at 400 K and under vacuum conditions. The peaks are assigned as follows: (a) the substrate MgO(002); (b) 5 nm Pd(001) cap; (c) 5 nm Fe(002) buffer layer; (d) 50 nm V(001) layer; (e) the same V(001) shifted under H pressure of 27 Pa.

makes the hydrogen atoms respond only to the hydrostatic stress component. This effect is seen in the hydrogen uptake in Fe/V(001) superlattices, in which the V layers are initially in a compressed biaxial strain state, resulting in an O_z site occupation in the α phase.[20] Based on these data we predicted that it is conceivable to obtain a reversible α-β phase transition in V(001) oriented thin films without degradation. The in-plane biaxial stress will be significantly smaller if only O sites are occupied, resulting in an expansion perpendicular to the film plane.

Here we present the results of *in situ* measurements of the lattice parameter and resistivity changes in thin vanadium films during exposure to hydrogen in a wide range of pressure and temperature. A fully reversible α-β phase transformation will be demonstrated, and the influence of the elastic boundaries on the thermodynamic properties will be discussed.

II. EXPERIMENT

The vanadium films were grown on polished MgO(001) single-crystal substrates with iron buffer layers below and above the V layer and a palladium cap layer using dc magnetron sputtering from separate Fe (of 99.95% purity), V (of 99.95% purity), and Pd (of 99.95% purity) targets. The growth conditions and sample characterization have been described in detail elsewhere.[21]

A specially designed x-ray scattering chamber was used for *in situ* resistivity and x-ray diffraction (XRD) measurements. The chamber body is made of UHV-compatible stainless steel. The x-ray beryllium windows are glued to the chamber body. A chromel-alumel thermocouple in contact with the sample surface is used to measure and control the sample's temperature (±0.1 °C) using a Eurotherm 2208 PID controller connected to a low-resistance radiative heater mounted inside the chamber. The pressure of the highly pure hydrogen was measured using two Inficon capacitance diaphragm gauges having full scales of 10 and 1000 torr (1.33×10^3 and 1.33×10^5 Pa), respectively. The accuracy of the pressure determination is 0.1% at full scale, and the precision was typically better than 0.1%. The resistivity of the sample was determined using a four-point probe and a Keithley 2400 sourcemeter in combination with a Keithley 2182 nanovoltmeter. The accuracy of the measured resistivity changes was governed by the temperature stability. X-ray reflectivity and diffraction were performed using a Bruker-AXS D8 Discover with a Cu source x-ray tube. The primary beam optics consists of a Göbel mirror in combination with a V-groove beam compressor, resulting in a parallel x-ray beam with a divergence smaller than 0.007° and a monochromatization ($\Delta\lambda/\lambda$) better than 0.01%. The diffracted beam was defined using an ordinary slit system. This system does not allow measurements of the in-plane diffraction. In-plane diffraction was made on the film after it was removed from the reactor. No significant changes were observed upon repeated hydrogen exposure.

Figure 1 demonstrates an XRD pattern of the 50 nm film at 400 K. All the relevant high-angle components of the film are represented: The MgO(001) oriented substrate (a), the (001) oriented Fe buffer and top layers (c), the Pd(001) textured capping (b), and the (001) oriented V layer (d). The MgO(002) peak was used as an internal reference for the determination of the peak positions for V, Fe, and Pd, which were within 0.6% of the values cited in the literature, 3.027, 2.8665, and 3.8898 Å, respectively.

As the H pressure in the chamber is increased, the V(002) peak is shifted, whereas all the other peaks remain unchanged, because only vanadium absorbs any significant amount of hydrogen under these experimental condition. The peak (e) represents the change in the vanadium diffraction line under hydrogen pressure of 27 Pa.

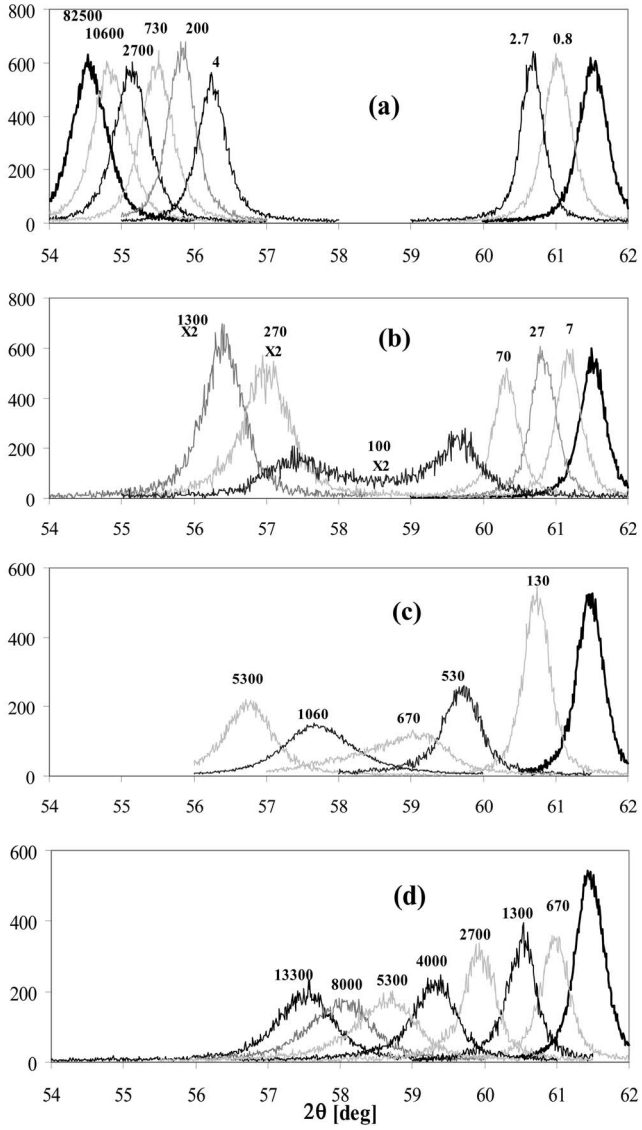

FIG. 2. Effect of hydrogen pressure and film temperature on the V(002) XRD peak of the 50 nm film. The intensity is in counts/s. The first peak on the right of each spectrum series was taken under vacuum conditions. Above each of the other peaks, the H pressure (in Pa) under which the spectrum was measured is shown. The temperatures of the film were (a) 380, (b) 440, (c) 480, and (d) 530 K.

III. RESULTS

A. Hydrogen-induced structural changes

The hydrogen-induced shift of the V(002) XRD line was measured *in situ* as a function of the hydrogen applied pressure for several temperatures. Some representative results are shown in Fig. 2. The first peak on the right of each spectrum series represents the initial (desorbed) state obtained by heating the sample and evacuating the scattering chamber. For each of the other XRD peaks, the hydrogen equilibrium pressure is indicated. It should be emphasized that the vanadium diffraction lines shown in Fig. 2 were completely reproducible. Each measured peak was obtained by first changing the H pressure, or the sample temperature, and then waiting until equilibrium was established. The time span required to reach equilibrium varied significantly. A small change in pressure in the vicinity of the plateau pressure required hours for reaching equilibrium, while otherwise equilibrium was obtained within a few minutes.

Figure 2(a) shows the pressure-dependent shift of the XRD peaks at 380 K, well below the ordering temperature for the bulk hydride. Maintaining the H pressure around 3 Pa, the peak above 60° gradually disappears while a peak below 60° simultaneously appears and increases in intensity. This is a clear indication of a phase transformation in the hydrogen-absorbing film. The difference between the lattice parameters of the pure vanadium and the new phase obtained from Fig. 2(a) corresponds to 0.22 Å, which is comparable to the expansion involved in the $\alpha \rightarrow \beta$ phase transformation of bulk V, i.e., 0.24 Å.[18] Figure 2(b) illustrates the corresponding changes close to the ordering temperature. Here, the separation between the two phases is less pronounced and a coexisting region is clearly seen. The observation of a two-phase region is ideally not expected under the present experimental conditions, i.e., equilibrium under excess of H gas. The existence of a two-phase region could result from a difference between the near-surface (and interfaces) and the interior regions of the film,[7] which is consistent with the decreased coherence length as seen by the broadening of the peaks. For even higher temperature, no two-phase region is found, though the peaks at the transition region are lower, wider, and asymmetric compared with the α-phase peaks as shown in Fig. 2(c). This may be the result of some overlapping of two wide but separated lines. The last series of pressure-dependent V(002) peaks shown in Fig. 2(d) was taken at 530 K, high above the critical temperature of the bulk phase. The peaks are shifted along with the H pressure, representing the disordered solid solution of hydrogen in vanadium, the α' phase.

B. Pressure isotherms based on the H-induced lattice expansion

The H-induced shifts of the V(002) XRD peaks shown in Fig. 2 are presented in Fig. 3 in the form of isotherms of the H pressure as a function of ε_H, the relative out-of-plane interplanar expansion of the film, for several temperatures. Here, ε_H is given by $\varepsilon_H=(\Delta d/d_0)_f$, where Δd is the H-induced expansion and d_0 is the H-free interplanar distance. Clearly, the data in Figs. 2 and 3 illustrate expansion below and above a critical temperature T_c. Above 480 K, the curves represent the isotherms for the disordered solid solution of H in the V(001) film, with a continuous shift of the (002) peak with pressure, corresponding to an α- α' transition. At and below 440 K, the isotherms demonstrate clear plateaus corresponding to an $\alpha \rightarrow \beta$ phase transition. Thus, the ordering temperature can be estimated as $T_c = 460 \pm 20$ K, with $P_c = 400 \pm 200$ Pa and $\varepsilon_{Hc} = 0.05$.

This determination is highly inaccurate and can easily be improved by additional measurements, which is beyond the scope of the current paper. However, the results are consistent with the data obtained for bulk V, for which the ordering temperature, obtained from differential thermal analysis

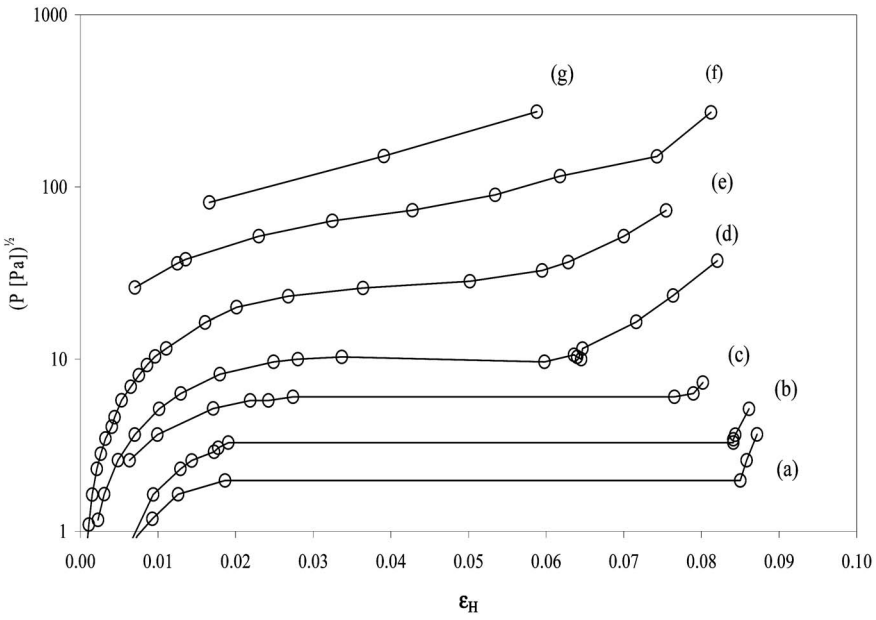

FIG. 3. Pressure isotherms for the 50 nm V film based on the H-induced out-of-plane lattice expansion. The experimental data points are calculated from the XRD shifts (see Fig. 2). The temperatures of the isotherms are (a) 380, (b) 400, (c) 420, (d) 440, (e) 480, (f) 530, and (g) 570 K.

measurements, is determined as 470 °K, at [H]/[V]=0.5.[22] The ordering temperature for hydride formation in thin films is typically lower than that of the bulk metal due to the limitations imposed on the volume expansion upon hydrogen absorption.[23] For a 100 nm Nb film[9] and for a 122 nm Pd film[23] the critical temperature decreases by 20%, whereas Nb films exceeding 500 nm,[9] and a 300 nm Pd film,[24] demonstrate bulklike behaviour. Hence, it is noteworthy that V(001) films as thin as 50 nm are rather bulklike concerning the V-H ordering temperature.

The plateau pressures $P_{\alpha\beta}$ shown in the isotherms of Fig. 3 below 440 K are associated with the phase transition

$$2(1-2x)^{-1}\mathrm{VH}_x\ (\alpha\ \text{phase}) + \tfrac{1}{2}\mathrm{H}_2 \leftrightarrows (1-2x)^{-1}\mathrm{V}_2\mathrm{H}\ (\beta\ \text{phase}). \quad (1)$$

Here x is the terminal solubility of hydrogen in the saturated α-phase V metal. The temperature dependence of these plateau pressures is given by[25]

$$R\ln(P_{\alpha\beta}/P_0)^{1/2} = \Delta H_{\alpha\beta}/T - \Delta S_{\alpha\beta}. \quad (2)$$

Here, $\Delta H_{\alpha\beta}$ and $\Delta S_{\alpha\beta}$ are the enthalpy and entropy of the transformation, respectively. The temperature dependence of the plateau pressures below the critical temperature is presented in Fig. 4 together with some cited representative data for bulk vanadium. The values obtained for $\Delta H_{\alpha\beta}$ and $\Delta S_{\alpha\beta}$ are -39 ± 1 kJ/mol K and -60 ± 2 J/mol, respectively. These values are in good agreement with those obtained for bulk V by several other authors,[26] which averaged to -38 ± 3 kJ/mol K for $\Delta H_{\alpha\beta}$ and -53 ± 5 J/mol for $\Delta S_{\alpha\beta}$. Thus, the similarity of the temperature dependence of the plateau pressures and the thermodynamic parameters for the hydride phase transition between bulk vanadium and the 50 nm film confirms the assigned phase transition in the film.

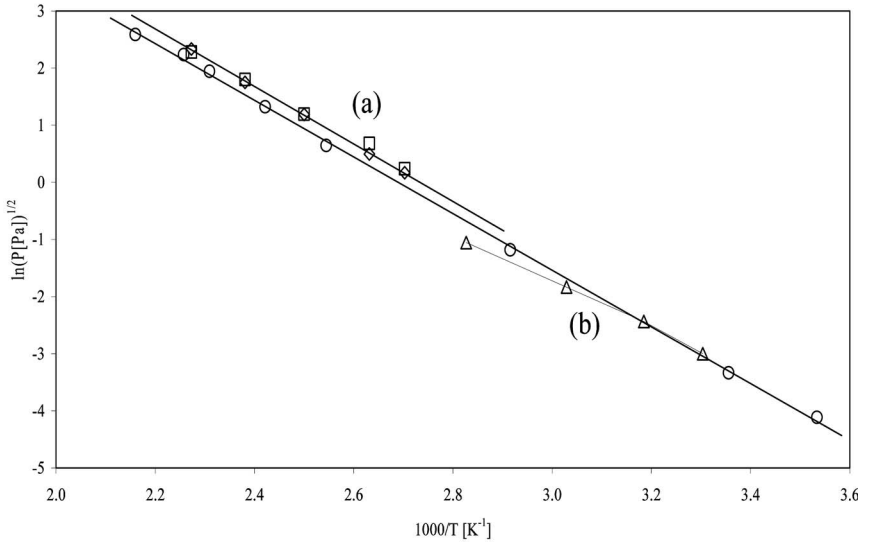

FIG. 4. van't Hoff temperature dependence of the plateau pressures in the V-H system for the following cases: (a) 50 nm V film: □, XRD results (Fig. 3); ◇, from resistivity measurements; (b) bulk V: ○, from Ref. 34; △, for 500 nm film (Ref. 26).

C. H-induced changes in the residual resistivity

The thermodynamic data presented in the previous section are solely based on the obtained XRD results. The changes in the resistivity have previously been used to determine the hydrogen concentration.[27,28] The maximum residual resistivity change, $\Delta\rho_{max}$, was determined to correspond to [H]/[V]=0.5.[28] Solubility isotherms for concentrations up to about 0.5 in [H]/[V] were constructed using the relation[28]

$$c_H = 0.5 \pm 0.5(1 - \Delta\rho/\Delta\rho_{max})^{1/2}. \quad (3)$$

The assumption that thin metallic films strictly obey Nordheim's rule is not always justified. Song *et al.* measured both P and $\Delta\rho$ versus ε_H for Nb thin films above T_c.[29] By comparing the pressure isotherms to the residual resistivity changes a pronounced deviation from the Nordheim rule was found. The evident asymmetry of the resistance curve produced $\Delta\rho_{max}$ at H concentrations much higher than at half the saturation concentration. Thus, they used a modified equation[30] to describe the concentration dependence of the resistivity:

$$\Delta\rho = A[a + (1-a)c_H]^2[c_H(1-c_H)] \quad (4)$$

with A and a as free parameters. The parameter a is related to the electron density in the H interstitial site.[30] Its value determines the degree of asymmetry of the excess resistivity for H in the metallic system. The smaller the value of a, the higher is the asymmetry. For $a=1$, the excess resistivity is symmetric about $c_H=0.5$ and Eq. (4) is substituted by Eq. (3). In Fig. 5, the pressure (P vs ε_H) and relative resistivity ($\Delta\rho/\Delta\rho_{max}$ vs ε_H) solubility isotherms of the V 50 nm film for two representative temperatures above T_c are compared. The excess resistivity maximum overlaps the point of inflection of the pressure isotherm. Assuming that the inflection point coincides with about half of the H saturation concentration and that the saturation concentration is $c_H=1$, it is obvious that the resistivity is symmetric about $c_H=0.5$, in contrast to the Nb case. The experimental data points of the resistivity isotherms shown in Fig. 5 were fitted using Eq. (4) with $a=1.04$, and $a=1.19$ for 480 and 530 K, respectively. It should be noticed that for Nb films the values obtained for a were very small: $a=0.01$ for 29 nm and $a=0.1$ for 140 nm films.[29] For H in Pd wires, Greeken and Griessen[30] have used the calculated value of the charge for the H site in the pure metal $a=0.21$.[31] There are two important conclusions from our results.

(1) The use of Eq. (3) (Nordheim's rule) for the analysis of thermodynamic parameters of H in thin V films[27,28] is justified.

(2) The equivalence of the thermodynamic behavior of a 50 nm V film to that of V bulk is confirmed.

It should be noted, however, that the assumption made above that the saturation concentration is $c_H=1$ is not straightforward. Comparison of the isotherms of V thin films[27] based on this assumption with isotherms of H in bulk V around 240,[32,33] 190, and 170 °C Ref. 34 shows that for bulk V the H concentration at the inflection point is $c_H=0.35$, 0.28, and 0.28, respectively, which is considerably smaller than $c_H=0.5$ assigned in the current results. This does not change the first conclusion above. Only the value of c_H at the maximum resistivity of the film (the inflection point of the pressure isotherm) should be calibrated to make the film and the bulk isotherms coincide.

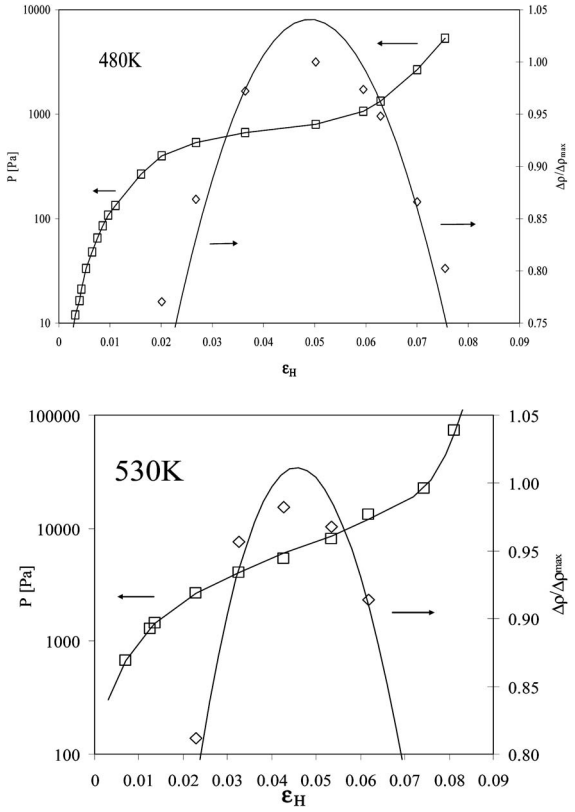

FIG. 5. Combined pressure (P vs ε_H) and resistivity ($\Delta\rho/\Delta\rho_{max}$ vs ε_H) solubility isotherms of the V 50 nm film for 480 (upper graph) and 530 K. Both cases are above T_c. The lines describing the resistivity isotherms were fitted using Eq. (4) with $a=1.04$, and $A=4.0$ for 480 K, and $a=1.19$ and $A=3.35$ for 530 K.

The relation between the resistivity maximum and the inflection point pressures (above T_c) or the plateau pressures (below T_c) for the film is shown in Fig. 6 which presents the pressure dependence of the excess resistivity of the 50 nm V film at different temperatures. Our results are in agreement with those of Andersson *et al.*[27] (curves *d* and *e* in Fig. 6). The inflection points of the pressure isotherms above T_c are indicated by arrows pointing upward. Arrows pointing downward denote plateau pressures associated with isotherms taken below T_c (see Fig. 3). There is an excellent match between the arrows (both above and below T_c) and the resistivity maxima.

The resistivity maximum $\Delta\rho_{max}$ is highly temperature dependent. Above the critical temperature it increases slightly with temperature as found also by Andersson *et al.*[27] Below T_c, however, the temperature effect is significantly stronger, reducing $\Delta\rho_{max}$ by a factor of 2 for a temperature drop from 480 to 380 K [compare curves (a) and (e) in Fig. 6]. Before discussing this subject in detail let us explore the results obtained for the 50 nm film below T_c. As noted above, a special feature of the system V(film)-H is the reversibility. This enables measurements over wide range of pressure and

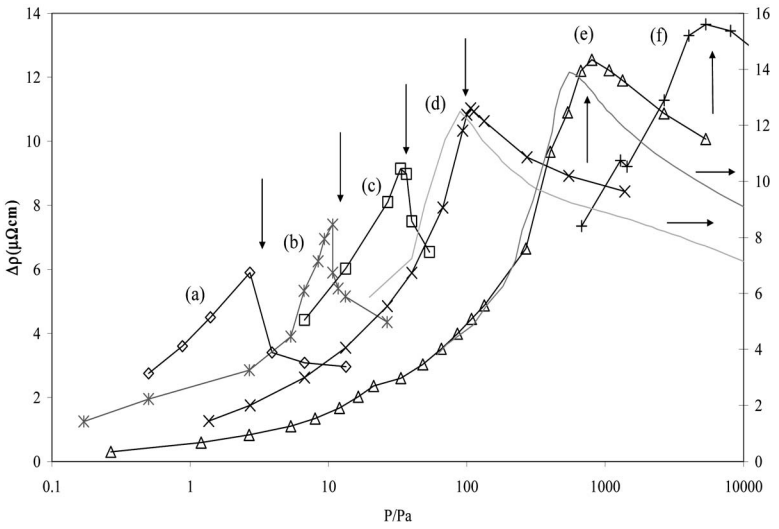

FIG. 6. Residual resistivity change as a function of the H pressure for the V 50 nm film for (a) 380 K, (b) 400 K, (c) 420 K, (d) 440 K (the light colored line was taken from Ref. 27 at 443 K), (e) 480 K (the light colored line was taken from Ref. 27 at 483 K), and (f) 530 K. The vertical arrows pointing upward show the pressure of the inflection point in the pressure isotherms and the arrows pointing down show the plateau pressures.

temperature as seen in Fig. 7, illustrating results obtained at temperatures below T_c. The two curves are complex: Three maxima and at least two minima are observed. The low-pressure maximum of the 370 K curve is a member of the series of maxima shown in Fig. 6, since it corresponds to the plateau pressure at this temperature. The origin of the higher-pressure peak is revealed in Fig. 8, in which the extended pressure ($P^{1/2}$ vs ε_H) and resistivity ($\Delta\rho/\Delta\rho_{max}$vs ε_H) isotherms at 380 K are combined. Assuming that the relative lattice parameter change, ε_H, is proportional to the H concentration c_H,[9] the pressure isotherm ($P^{1/2}$ vs ε_H) can be divided into three regions: (1) the low H concentration range (up to $\varepsilon_H=0.02$) corresponding to H solubility in the α phase; (2) the plateau range ($0.02<\varepsilon_H<0.085$) associated with a phase transition; and (3) a higher-concentration range, above the plateau, corresponding to H dissolution in the new phase, giving rise to a characteristic high-temperature (above T_c) isotherm.

It is clear from Fig. 8 that the second maximum of the resistivity coincides with the inflection point apparent in the third region of the pressure isotherm.

D. The $\alpha \rightarrow \beta$ phase transition

The reversible phase transition demonstrated in Figs. 2 and 3 for $T<T_c$ is attributed to a bulklike $\alpha \rightarrow \beta$ phase transformation because the observed plateau pressures and T_c are similar to those of bulk V. Further confirmation is presented in Table I, comparing lattice parameters of some V-H phases for the 50 nm film and for bulk V at 380 K.

The values for bulk V were retrieved from Maeland[18] either directly or by using the reported temperature coefficients of expansion where possible. The lattice constants for the 50 nm V film were obtained using the MgO(002) peak as an internal reference (see Sec. II). The lattice parameters of the film and the bulk V are almost the same, as shown by the values of d_{bulk}/d_{film}, which are very close to unity. The difference is less than 1% for the β phase and is much smaller for the other structures. Considering experimental errors it seems evident that the V-H system is identical for the bulk and the 50 nm film. The value of $c_H=0.15$ for the $\alpha_{saturated}$ case is obtained from Maeland (Fig. 3 in Ref. 18). This value is in agreement with the result for the 50 nm film. The terminal H solubility reported for V bulk[35] is lower than in the

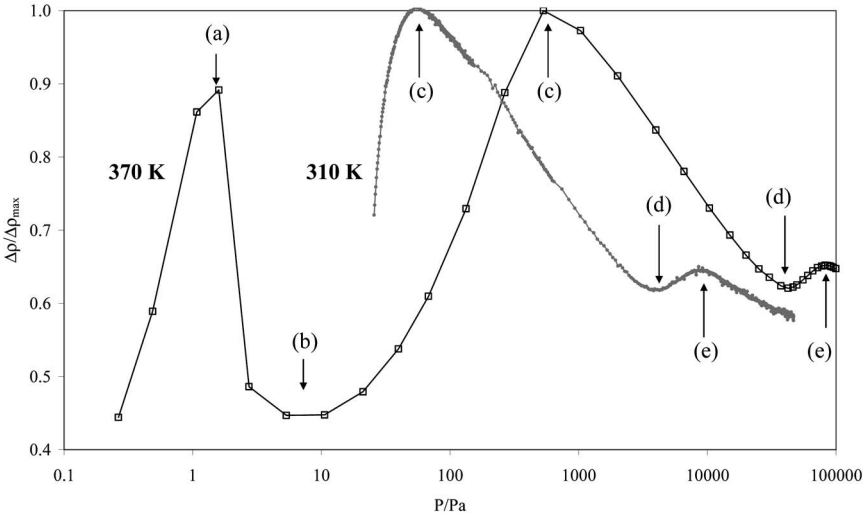

FIG. 7. Relative change of the residual resistivity as a function of the H pressure in the V 50 nm film for two indicated temperatures below the $\alpha \rightarrow \beta$ critical temperature. The maxima and minima are assigned according to the V phase diagram (Ref. 22). (a) Initiation of the $\alpha \rightarrow \beta$ phase transformation at the solvus line; (b) the complete formation of the β phase; (c) half of the O_{z2} interstitial sites are occupied; (d) and (e) see text.

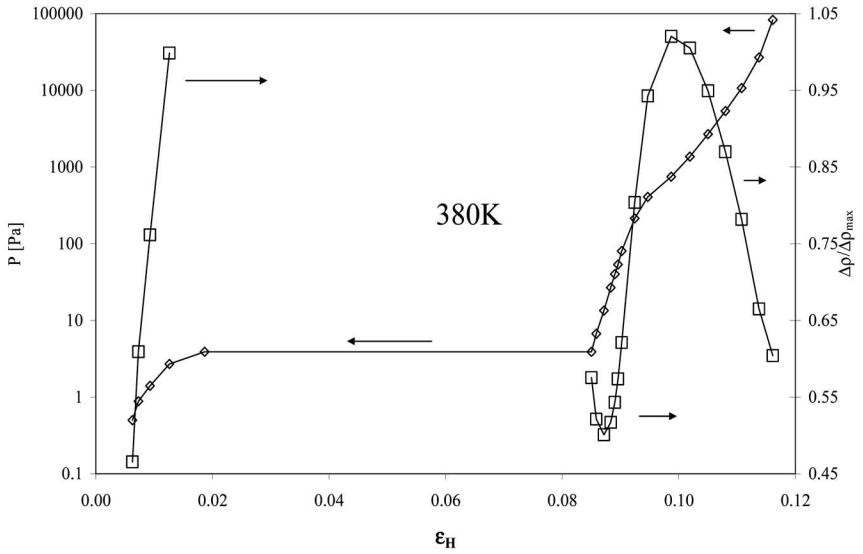

FIG. 8. Combined pressure (P vs ε_H) and relative resistivity change ($\Delta\rho/\Delta\rho_{max}$ vs ε_H) solubility isotherms of the V 50 nm film at 380 K.

film (around 0.1). In Table I, however, the lattice expansions are compared for the same H concentration. The values presented for the lattice expansions of the β phases in the bulk V are for 300 K.[18]

For the film the expansion was measured from the β peak which is the first to appear at the initiation of the transformation [see Fig. 2(a)]. The composition of the β phase is believed to be $VH_{0.5}$.[1,2,18] In order to obtain a better evaluation we correlated and scaled that part of our ($P^{1/2}$ vs ε_H) isotherm at 380 K shown in Fig. 8, which comprises the concentration range above the plateau, with $P^{1/2}$ vs c_H isotherms reported for bulk V at 343 (Ref. 36) and at 373 K.[35] Good agreement between the bulk V and 50 nm film isotherm is obtained assuming c_H=0.46 for the pure β phase. According to the above correlation, the highest H concentration achieved was c_H=0.72 (at 300 K Maeland[18] assigned c_H=0.8 for the β saturation concentration). We have used this value to compare the bulk V and the film lattice expansions of the $\beta_{saturated}$ structure.

In conclusion, the data shown in Table I indicate very small differences between the absolute values of the lattice parameters in the bulk and the 50 nm V film.

IV. DISCUSSION

The similarity of the bulk and 50 nm V film regarding the H absorption thermodynamics and the hydride lattice structure can be used to clarify some of the features of the multiple-maxima resistivity isotherm ($\Delta\rho/\Delta\rho_{max}$ vs $P^{1/2}$) shown in Fig. 7 and the combined pressure ($P^{1/2}$ vs ε_H) and resistivity ($\Delta\rho/\Delta\rho_{max}$ vs ε_H) isotherms shown in Fig. 8. We explain those features according to previously published data concerning the thermodynamics and the phase diagram of the bulk V-H system. Below 400 K and under 1 bar H_2, two plateaus are observed in the pressure-composition isotherms of H in bulk V. The first is extended up to $c_H \approx 0.5$, and corresponds to the $\alpha \rightarrow \beta$ phase transformation. The second plateau has an inflection point at around c_H=0.65,[36] and is completed near $c_H \approx 0.8$.[26,34,36] We assume that this second plateau coincides with our second plateau of the ($P^{1/2}$ vs ε_H) isotherm shown in Fig. 8. This plateau is associated with the $\beta \rightarrow \beta'$ (or ε) order-disorder transition,[2,19] sometimes assigned as $\beta_1 \rightarrow \beta_2$ transition.[37,38] Above around 480 K the first and second plateaus join together.[35,39] It has been shown above (Figs. 5 and 8) that the (a) maximum of the resistivity curve in Fig. 7 coincides with inflection point above T_c or with the first appearance of the plateau below T_c. Similarly, the (c) maximum of the resistivity curve in Fig. 7 probably coincides with the inflection point of the second plateau as shown in Fig. 8.

Another source of data available for explaining the significance of the features shown in Figs. 7 and 8 is the V-H phase diagram[22,37] constructed with the results of several workers using thermal desorption and neutron and x-ray diffraction techniques. Drawing isothermal lines at 370 and at 310 K along the H concentration axis on the V-H phase

TABLE I. Lattice parameters (in Å) of some V-H phases in the forms of a 50 nm film and bulk V (Ref. 18) at 380 K.

Phase	c_H ([H]/[V])	d_{bulk} (Ref. 18)	d_{film} (±0.002 Å)	d_{bulk}/d_{film} (±0.003 Å)	$\Delta d/d_0$ (bulk)	$\Delta d/d_0$ (film) (±0.01 Å)
α	0	3.028	3.018	1.003		
$\alpha_{saturated}$	0.15	3.064	3.060	1.001	0.01	0.01
$\beta(c_0)$	0.5	3.302	3.274	1.009	0.09	0.09
$\beta_{saturated}$	0.72	3.380	3.362	1.005	0.12	0.11

diagram[22] reveals the following vertical boundaries.

(1) The α-phase solvus separating the α and the $\alpha+\beta$ regions at around $c_{H(370\ K)}=0.09$ and $c_{H(310\ K)}=0.025$. The solvus line has significant temperature dependence. For the film the values of the terminal solubility are higher, as shown above ($c_{H(370\ K)}=0.13$ and $c_{H(310\ K)}=0.05$; see Fig. 8).

(2) The phase boundary $\alpha+\beta\rightarrow\beta$ between the two- and the single-phase regions at around $c_{H(370\ K)}=0.47$. This boundary line is almost temperature independent.[22]

(3) A phase boundary $\beta\rightarrow\beta'$ at around $c_{H(370\ K)}=0.65$. Here the temperature dependence is also relatively weak. Notice that, in contrast to the $\alpha\rightarrow\beta$ first-order phase transition, the $\beta\rightarrow\beta'$ transition is a second-order transformation, in agreement with the *p-c-T* data showing an inflection point instead of a real plateau in this range.

(4) The first-order $\beta'\rightarrow\beta'+\gamma$ transformation where γ is the VH_2 fcc phase. The location of the boundary is uncertain, but it must be around $c_H=1$.

To analyze the resistivity-pressure curve according to the *p-c-T* and phase diagram data, it is assumed that H atoms randomly added into an ordered system such as a metal crystal may increase its resistivity, because the arbitrarily distributed H atoms serve as scattering centers. On the other hand, when H interstitials are incorporated in an ordered way, the resistivity is decreased. A minimum will appear in the ΔR vs $P^{1/2}$ isotherm when the ordered occupation of the interstitials is completed.

Based on this description the complex multiple-maxima structure of Fig. 7 can be explained.

(1) Initially, the resistivity is increased because of H dissolved in the α phase. The H atoms randomly occupy the tetrahedral interstices. The first maximum, (a) in Figs. 7 and 8, appears as the α terminal solubility is reached and the β phase starts to form. Thus, this maximum is associated with the $\alpha\rightarrow\alpha+\beta$ phase transition.

(2) The sharp drop from the (a) maximum to the (b) minimum in Fig. 7 corresponds to the phase transformation $\alpha\rightarrow\beta$ along the $\alpha+\beta$ two-phase region. The change is sharp because this transition is taking place under constant (equilibrium) H pressure at $T<T_c$. In the β phase the H atoms occupy the O_{z1} interstices in an ordered way; hence the resistivity is decreased. A minimum is achieved at the complete formation of the β phase. The value of $\Delta\rho/\Delta\rho_{max}$ at the (b) minimum is still almost two times higher than that of the pure metal. Pryde and Tsong[40] have found a similar sharp minimum in the resistivity-concentration curve of tantalum filament around $TaH_{0.5}$, attributed to the formation of a superlattice of H atoms (comparable to the V β phase) in the metal. The formation of such a superlattice in a very thin film, like ours, is likely as well. This minimum is expected to overlap with the far edge of the $\alpha\rightarrow\beta$ transition plateau. In Fig. 8, however, it is shown that it is somewhat shifted beyond the end of the plateau. Apparently, H atoms continue to occupy periodic sites in the β phase immediately after its formation. This shift may indicate increase of the H concentration from $c_H=0.47$ to $c_H=0.5$.

(3) At the (b) minimum the formation of the ordered β phase is complete. Next, H atoms randomly enter the O_{z2} interstices, increasing the resistivity toward the (c) maximum.

(4) At the (c) maximum all the O_{z1} and half of the O_{z2} interstices are occupied by H atoms. The maximum coincides with the isotherm's inflection point as shown in Fig. 8. Again, a similar maximum has been found for the Ta-D system,[40] associated with the occupation of half of the available H sites between $TaD_{0.5}$ and TaD. Around this concentration, however, the Ta filament has failed. Comparing the resistivity-pressure isotherm of the 50 nm film with *p-c-T* data[34,36] of bulk V suggests that the (c) maximum coincides with the inflection point corresponding to the $\beta\rightarrow\beta'$ transition at $c_{H(370\ K)}=0.65$.

(5) Following the (c) maximum the resistivity decreases because, when more than half of the available interstices are occupied, the system is approaching the ordered V state, in which all the available octahedral (both O_{z1} and O_{z2}) interstices are occupied.

(6) The (d) minimum and the (e) maximum in Fig. 7 have no counterpart in the bulk V phase diagram and are characteristic of the 50 nm film. According to the phase diagram one would expect the resistivity to go down to a point around $c_H=1$ where the γ phase (VH_2) is formed. However, the plateau pressure for the $\beta'\rightarrow\beta'+\gamma$ transformation at 310 K is 5×10^5 Pa,[41] much higher than the pressure 4×10^3 Pa shown for the (d) minimum at 310 K in Fig. 7. Thus, it cannot be attributed to the $VH\rightarrow VH_2$ transformation. It should be mentioned that Asano *et al.*[38] assumed that the H atoms in the β' phase are distributed in all the O_z interstices with equal probability, because the β' phase is the high-temperature form of the β phase. For the 50 nm V film, however, the isothermal transition from the β ($VH_{0.5}$) to the β' (VH) phase involves another order-disorder transition. We suggest that, when the O_{z2} interstices are filled to a certain temperature-dependent concentration, some H atoms move from O_{z1} to O_{z2} interstices along with the penetration of H atoms from the gas phase, increasing the number of randomly distributed H atoms and hence the film resistivity. The (e) maximum is then achieved when the maximum degree of random distribution of the H atoms in both O_{z1} and O_{z2} interstices is accomplished.

According to a simple model developed by Pryde and Tsong[40] for high-concentration interstitial alloys, the maximum value of the excess resistivity, $\Delta\rho_{max}$, occurs at $c_H=1/2c_{H\ max}$. Here $c_{H\ max}=N_s/N_m$ where N_s is the total number (filled and empty) of interstitial sites per unit volume and N_m is the number of metal atoms per unit volume. Thus $\Delta\rho_{max}$ is given by

$$\Delta\rho_{max}=KN_mc_{H\ max}. \tag{5}$$

K is a constant depending among other things on the difference between the potentials within the occupied and empty H interstitial sites. For the Ta-D system[40] it has been assumed that minima in $\Delta\rho$ occur at the ordered compositions $TaD_{0.5}$ and TaD, and a maximum rises between them at $TaD_{0.75}$, the height of which is one-half of $\Delta\rho_{max}$ for the high-temperature disordered α-phase region, because $c_{H\ max}$ is reduced from 1 to 0.5. For the 50 nm V film the value of $\Delta\rho_{max}$ at the (c) maximum above T_c (around 460 K) is weakly temperature dependent.[27]. This is shown in curves (e) and (f) of Fig. 6. At

this temperature range there is only one plateau, $c_{H\,max}=1$, and $\Delta\rho_{max}$ appears at $c_H \approx 0.5$. Below T_c, however, the (c) maximum corresponds to the difference between the amounts of interstices in the ordered phases β ($VH_{0.5}$) and β' (VH), i.e., $c_{H\,max}=0.5$. Hence, the height of the maximum should be one-half of the high-temperature maximum, in accordance with the change in $c_{H\,max}$ from 1 to 0.5 in Eq. (5). This change with temperature is evident in Fig. 6 and it is similar to the results obtained for the Ta-H system mentioned above.[40] It is expected that, for temperatures lower than those shown in Fig. 6, $\Delta\rho_{max}$ will approach a constant value.

The similarity of the values of $\Delta\rho_{max}$ of the (a) and (c) maxima below T_c as shown in Fig. 7 suggests that $c_{H\,max}$ is approximately 0.5 for the (a) maximum. It is tempting to relate this value to the β ($VH_{0.5}$) phase. However, it seems that the (a) maximum corresponds to the unclear value of $c_{H\,max}$ in the α phase. Theoretically there are as many as 6 tetrahedral sites in the bcc lattice. However, experimental thermodynamic results at high temperatures could be fitted only with much smaller $c_{H\,max}$ values, ranging from 0.78 (Ref. 32) to 0.35,[27], in agreement with the value found for the 50 nm V film.

V. SUMMARY AND CONCLUSIONS

The thermodynamics of H absorption and the associated structural changes were studied using combined XRD and residual resistivity changes for a 50 nm V(001) film grown on MgO(001) with a Fe(001) buffer layer. A thin film of a single element was found which exhibits completely reversible hydrogen-induced phase transformations.

(1) A bulklike first-order $\alpha \rightarrow \beta$ ($VH_{0.5}$) transformation. The critical temperature for this phase transformation is 460 ± 20 K.

(2) A second-order $\beta \rightarrow \beta'$ transition corresponding to the occupation of O_{z2} interstitials.

(3) An unidentified additional second-order transition taking place at $0.67 < c_H < 1.0$. This transition has not been observed in bulk samples to our knowledge.

The thermodynamic constants for the $\alpha \rightarrow \beta$ phase transformation in the film are $\Delta H_{\alpha\beta}=-39\pm1$ kJ/mol °K, $\Delta S_{\alpha\beta}=-60\pm2$ J/mol, and $T_c=460\pm20$ K, similar to those of bulk V (38 ± 3 kJ/mol °K for $\Delta H_{\alpha\beta}$, and -53 ± 5 J/mol for $\Delta S_{\alpha\beta}$, and $T_c=470$ K).

The H concentration dependence of the residual resistance change of the V film generally includes several minima and maxima. The first maximum, ΔR_{max}, coincides with the inflection point of the pressure isotherm for temperatures above T_c of the $\alpha \rightarrow \beta$ transformation, and with the initiation of the β-phase formation below T_c. Thus, ΔR_{max} corresponds to the terminal solubility of H in the α phase. The value of ΔR_{max} increases with temperature as the value of $c_{H\,max}$, the maximal H concentration, is changing from 0.5 below to 1 above the critical temperature. These results clearly show how thin films can be used to explore the hydrogen-induced changes in the physical properties of metals.

*Permanent address: Nuclear Centre-Negev, P. O. Box 9001, Beer-Sheva, Israel.

[1] T. Schober and H. Wenzl, in *Hydrogen in Metals II*, edited by G. Alefeld and J. Völkl, Topics in Applied Physics Vol. 29 (Springer, Berlin, 1978), Chap. 2.
[2] T. Schober, in *Hydrogen Metal Systems I*, edited by F. A. Lewis and A. Aladjem, Solid State Phenomena Vols. 49-50 (Scitec, Zurich, 1996), Chap. 9.
[3] H. Zabel and B. Hjörvarsson, in *Progress in Hydrogen Treatment of Materials*, edited by V. A. Goltsov (Donetsk, Coral Gables: Kassiopeya, 2001), p. 119.
[4] P. F. Miceli, H. Zabel, and J. E. Cunningham, Phys. Rev. Lett. **54**, 917 (1985).
[5] J. Steiger, S. Blässer, and A. Weidinger, Phys. Rev. B **49**, 5570 (1994).
[6] B. Hjörvarsson, J. Rydén, E. Karlsson, J. Birch, and J.-E. Sundgren, Phys. Rev. B **43**, 6440 (1990).
[7] G. Andersson, B. Hjörvarsson, and P. Isberg, Phys. Rev. B **55**, 1774 (1997).
[8] G. Reisfeld, N. M. Jisrawi, M. W. Ruckman, and M. Strongin, Phys. Rev. B **53**, 4974 (1996).
[9] G. Song, M. Geitz, A. Abromeit, and H. Zabel, Phys. Rev. B **54**, 14093 (1996).
[10] P. M. Reimer, H. Zabel, C. P. Flynn, A. Matheny, K. Ritely, J. Steiger, S. Blässer, and A. Weidinger, Z. Phys. Chem. **181**, 367 (1993).
[11] G. Song, A. Remhof, K. Theis-Bröhl, and H. Zabel, Phys. Rev. Lett. **79**, 5062 (1997).
[12] P. F. Miceli, H. Zabel, J. A. Dura, and C. P. Flynn, J. Mater. Res. **6**, 964 (1991).
[13] Q. M. Yang, G. Schmitz, S. Föhler, H. U. Krebs, and R. Kirchheim, Phys. Rev. B **54**, 9131 (1996).
[14] H. Sugimoto and Y. Fukai, Phys. Rev. B **22**, 670 (1980).
[15] A. Yu. Chervyakov, I. R. Entin, V. A. Somenkov, S. Sh. Shil'shtein, and A. A. Chertkov, Sov. Phys. Solid State **13**, 2172 (1972).
[16] V. A. Somenkov, I. R. Entin, A. Yu. Chervyakov, S. Sh. Shil'shtein, and A. A. Chertkov, Sov. Phys. Solid State **13**, 2178 (1972).
[17] T. Suzuki, H. Namazue, S. Koike, and H. Hayakawa, Phys. Rev. Lett. **51**, 798 (1983).
[18] A. J. Maeland, J. Phys. Chem. **68**, 2197 (1964).
[19] H. Asano and M. Hirabayashi, Phys. Status Solidi A **15**, 267 (1973).
[20] G. Andersson, B. Hjörvarsson, and H. Zabel, Phys. Rev. B **55**, 15905 (1997).
[21] J. Bloch, B. Hjörvarsson, S. Olsson, and R. Brukas (unpublished).
[22] W. Pesch, T. Schober, and H. Wenzl, Scr. Metall. **16**, 307 (1982).
[23] R. Feenstra, G. J. de Bruin-Hordijk, H. L. M. Bakker, R. Griessen, and D. G. de Groot, J. Phys. F: Met. Phys. **13**, L13 (1983).
[24] E. M. Salomons, R. Feenstra, D. G. de Groot, J. H. Rector, and R. Griessen, J. Less-Common Met. **130**, 415 (1987).

[25] P. S. Rudman, Int. J. Hydrogen Energy **3**, 431 (1978).
[26] K. Papathanassopoulos and H. Wenzl, J. Phys. F: Met. Phys. **12**, 1369 (1982).
[27] G. Andersson, K. Aits, and B. Hjörvarsson, J. Alloys Compd. **334**, 14 (2002).
[28] F. Stillesjö, S. Ólafsson, P. Isberg, and B. Hjörvarsson, J. Phys.: Condens. Matter **7**, 8139 (1995).
[29] G. Song, A. Remhof, D. Labergerie, and H. Zabel, Phys. Rev. B **66**, 045407 (2002).
[30] B. M. Greeken and R. Griessen, J. Phys. F: Met. Phys. **13**, 963 (1983).
[31] C. D. Gelatt, H. Ehrenreich, and J. A. Weiss, Phys. Rev. B **17**, 1940 (1978).
[32] E. Veleckis and R. K. Edwards, J. Phys. Chem. **73**, 683 (169).
[33] S. Hayashi, J. Alloys Compd. **359**, 281 (2003).
[34] R. Griffiths, J. A. Pryde, and A. Righini-Brand, J. Chem. Soc., Faraday Trans. 1 **68**, 2344 (1972).
[35] K. Fujita, Y. C. Huang, and M. Tada, Nippon Kinzoku Gakkaishi **43**, 601 (1979).
[36] H. Yukawa, D. Yamashita, S. Ito, M. Morinaga, and S. Yamaguchi, J. Alloys Compd. **356-357**, 45 (2003).
[37] F. D. Manchester, J. Alloys Compd. **330-332**, 8 (2002).
[38] H. Asano, Y. Abe, and M. Hirabayashi, Acta Metall. **24**, 95 (1976).
[39] P. Meuffels, KFA-Julich Report No. 2081, 1986 (unpublished).
[40] J. A. Pryde and I. S. T. Tsong, Acta Metall. **19**, 1333 (1971).
[41] R. H. Wiswall and J. J. Reilly, Inorg. Chem. **11**, 1691 (1972).